

# Possible Extragalactic Origins of Five LMC Globular Clusters: Proper Motion Deviations in *Gaia* DR3

Tamojeet Roychowdhury<sup>1</sup><sup>\*</sup> and Navdha<sup>1</sup>

<sup>1</sup>India Institute of Technology, Bombay, Mumbai, India - 400076

Accepted XXX. Received YYY; in original form ZZZ

## ABSTRACT

We use kinematic data of proper motions from *Gaia* of forty-two globular and open clusters from Large Magellanic Cloud (LMC) to explore the possibility of them having extragalactic origins. We find the difference between the proper motions of cluster stars and a surrounding patch of young LMC stars in each case. We find five globular clusters towards the north-east showing a high difference ( $> 0.11$  mas/yr, or  $> 25$  km/s). We also examine the statistical significance of this difference taking into account both measurement errors of cluster and surrounding stars as well as inherent dispersion of stellar motions in the local galactic environment. The five globular clusters (NGC 2005, NGC 2210, NGC 1978, Hodge 3 and Hodge 11) have mean proper motions that lie outside the 85% confidence interval of the mean of surrounding young stars, with a clear outlier (NGC 1978 outside 99.96% confidence) whose difference cannot be accounted for by statistical noise. A young cluster (NGC 2100) also fitting the criteria is ruled out owing to contrary evidence from literature. This indicates a possible interaction with a dwarf galaxy resulting in the accretion/disruption in path of the five globular clusters, or possibly one or more past merger(s) of smaller galaxy/galaxies with LMC from its north-eastern region. This direction also coincides with the location of Tarantula Nebula, suggesting the possibility of the interaction event or merger having triggered its star formation activity.

**Key words:** galaxies: globular clusters – galaxies: Magellanic Clouds – galaxy: kinematics and dynamics

## 1 INTRODUCTION

The Large Magellanic Cloud (LMC) is Milky Way's largest satellite galaxy and has several smaller satellite galaxies itself as shown in Erkal & Belokurov (2020), Patel et al. (2020) - but so far the only known sign of interaction between LMC and any of its satellites is with the Small Magellanic Cloud.

Mucciarelli et al. (2021) showed via chemical analysis that the globular cluster NGC 2005 most likely did not originate within LMC, indicating a past merger event in the galaxy. These mergers can be traced by kinematic signatures, specifically by using the difference of the observed stellar motions vs the expected stellar motions with respect to the galaxy. Accurate kinematic properties obtained from *Gaia* has further been used to find tidal tails of clusters - for instance in Sollima (2020), characterization of the Sagittarius stream in Ramos et al. (2022), and has helped map nuances of the Milky Way galaxy in general. Phase space information has also been used to uncover the merger of *Gaia*-Enceladus into the Milky Way by Helmi et al. (2018a). Several globular clusters of the Milky Way have been shown to originate from past merger events and interactions with the closely orbiting Sagittarius Dwarf in Massari et al. (2019). These instances demonstrate the potential of *Gaia*'s accurate astrometric measurements in determining galactic structure and history, as well as of globular clusters to carry signatures of the galaxy's past in these measurements.

Moreover, Pagnini et al. (2023) showed that globular clusters from

accreted galaxies can dwell in locations populated by stars from a different progenitor including *in-situ* formation. We thus use this to argue that young blue stars in a region around the globular cluster must have formed *in-situ*, and if the globular cluster is accreted or perturbed by interactions, it will have a slightly different motion from the young blue population.

Since *Gaia* DR3 does not have radial velocity measurements of stars as far as LMC, we chose to use only the proper motion of the stars. A relatively large number of clusters were studied in order to analyze the effects of considering only the proper motion (instead of the full velocity).

Mean proper motions for clusters alone within the Milky Way has been derived to a high accuracy in Helmi et al. (2018b), and later in Vasiliev (2019). The latter also details the presence of spatially correlated systematic errors in *Gaia*'s proper motions, as well as the effect of random errors. These need to be accounted for before we analyze the differences in mean proper motion. Kinematic properties of several globular clusters of LMC were analyzed to a high accuracy by Bennet et al. (2022) with combined data from *Gaia* and Hubble. They also derived the galaxy rotation dynamics using the data of *cluster motions alone*, and found a relation using it. What we propose to do is to obtain a measure of the *difference* between the proper motion of the globular clusters with that of the surrounding stars. To the best of our knowledge, such an analysis has not been conducted in earlier works.

We derive the mean proper motion of the cluster ourselves and compare those against the values reported in the above paper. Bennet et al. (2022) also reported NGC 2210 as a likely extragalactic member

\* E-mail: tamojeet@iitb.ac.in (IITB)

in LMC, apart from NGC 2005 reported in [Mucciarelli et al. \(2021\)](#). Our analysis finds them both to be outsiders too, apart from three more clusters. One of these is NGC 1978, whose peculiar elliptical shape was ascertained by [Mucciarelli et al. \(2007\)](#) suggesting the possibility of it having been accreted from outside the galaxy followed by tidal distortion. The two other clusters, Hodge 3 and Hodge 11, are old globular clusters, taken from [Olszewski et al. \(1996\)](#) and if not accreted from outside, their kinematic properties may have been influenced by past interactions with the SMC or other dwarf galaxies. Multiple stellar populations have been detected in Hodge 11 and NGC 2210 in [Gilligan et al. \(2019\)](#). One possible explanation for these, given by [Helmi \(2008\)](#) is that these globular clusters are remnants of cores of accreted dwarf galaxies, which was also explored for Messier 54 globular cluster in Sagittarius Dwarf by [Carretta et al. \(2010\)](#). This would then be consistent with our claim of their extragalactic origin. The last member, NGC 2100, is itself a young cluster located in the Tarantula Nebula but presents a significant difference of proper motion w.r.t. its neighbourhood. However, evidence from prior literature points against the likelihood of its accretion.

In the following sections we present our data selection criteria, the method for quantifying the proper motion differences, checking for effects of errors and results for the sample of clusters chosen.

## 2 DATA SELECTION

Most clusters are chosen from the New General Catalog of [Dreyer \(1888\)](#). ESO 57-30 is from the catalog in [Bica et al. \(1999\)](#). Hodge 3 and 11 were originally listed in [Hodge & Wright \(1967\)](#). We specifically looked for NGC clusters within a  $5^\circ$  circle around the LMC centre coordinates taken as (RA, Dec) = (80.8942, -69.756) by performing a SIMBAD search for the same, and supplemented it with clusters taken from the list of [Olszewski et al. \(1996\)](#) (which has old globular clusters) and [Bennet et al. \(2022\)](#) (which does a similar proper motion analysis).

We use high-quality proper motion data from *Gaia* DR3 described in [Gaia Collaboration \(2016\)](#) and [Gaia Collaboration \(2022\)](#). We first retrieved the bulk of LMC stars using the following criteria:

- Stars must lie within a  $5^\circ$  circle around the LMC centre coordinates taken as (RA, Dec) = (80.8942, -69.756). The  $5^\circ$  radius was chosen as a rough measure of the point till where LMC stars still dominate over field star population.
- Stars with no proper motion measurement in DR3 are removed
- Stars with poor astrometric data are removed, by selecting only those stars with Renormalized Unit Weight Error (RUWE)  $< 1.4$ . This gives the optimal selection of stars with accurate astrometric solutions, as shown in [Lindgren et al. \(2018\)](#)
- Stars with well-known (RUWE  $< 1.4$ ) parallaxes above 0.1 mas (corresponding to distances less than 10 kpc) are also removed, as these correspond to line-of-sight contamination by LMC non-members

We now obtain similar data of both open and globular clusters and their surrounding patches. The following approach was adopted:

- Only stars with RUWE  $< 1.4$  and parallax  $< 0.1$  mas are retained as in the previous case
- For cluster stars, the cluster centre coordinates are obtained from SIMBAD, and a region of 0.03 degree radius centred on those coordinates is queried from. The choice for 0.03 degree is explained in subsection 2.2
- Any cluster with less than 85 stars in the 0.03 degree disc is removed, to reduce estimation errors discussed in Section 3

- For surrounding stars, all stars with a radius  $> 0.05$  degrees and  $< 0.25$  degrees (again explained in subsection 2.2), centred at the cluster centre are queried for

The reason for picking both globular and open clusters is to use as large a sample as possible, to demonstrate that high differences are not properties of typical clusters in LMC (details in Section 3).

The outer annulus radius is slightly varied, at 0.18 degrees for dense regions near the centre for seven clusters (to reduce the size of the local environment where the mean proper motion is being measured, since central regions have larger velocity variations on a similar spatial scale), 0.28 degrees for NGC 2210 and 0.45 degrees for NGC 2203 (which lie in sparser regions of the galaxy and did not have a large enough sample of outer blue stars to analyze). The radius was optimized for these cases to include sufficient number of stars to return a good Gaussian fit (curve-fitting error in mean  $< 1\%$ ).

Since we are observing LMC from outside and at a significant distance, correction for solar reflex proper motion, which was necessary for the proper motions of Milky Way stars in [Helmi et al. \(2018a\)](#), is not needed in this work.

Additionally, we observe that due to *Gaia*'s limiting magnitude of around 21, only the red giant stars and blue giant stars of the Hertzsprung-Russell (HR) diagrams are retrieved, and any lower main sequence and white dwarfs remain hidden. Since we wish to find the difference of a cluster's stars' proper motion with the galaxy's own stars that formed *in-situ*, we chose to retain only the blue giant branch members of the surrounding stars, since these are young stars that are less likely to have been accreted in an interaction/merger event from a different galaxy. For these stars we have the difference between the blue and red passband magnitudes,  $G_{BP} - G_{RP} < 0.75$  (obtained empirically by observing the HR diagrams for the samples obtained). We hence use this criteria as a filter for a cluster's surrounding blue stars. We now discuss possible sources of errors inherent in the data and analyze their effects on our results.

### 2.1 Measurement Errors

*Gaia*'s proper motions are expected to have a naturally arising error in measurement. A spatially correlated systematic error is outlined in [Lindgren et al. \(2018\)](#), and later shown to be the dominant cause of error (at least for clusters with  $\gtrsim 100$  members, which was imposed as part of our data selection criteria) in Milky Way globular clusters in their kinematic analysis by [Vasiliev \(2019\)](#), at a value of about 0.08 mas/yr. These systematic errors are spatially correlated and can effectively be considered as zero-point offsets within  $1^\circ$  regions - as used in analysis of ultra-faint dwarfs in [Battaglia et al. \(2022\)](#), based on the *Gaia* EDR3 astrometry outlined in [Lindgren et al. \(2021\)](#), implying that this offset error for each globular cluster and its surrounding LMC star field, within a circle of  $0.25^\circ$  radius, would have identical values. Since we are attempting to quantify only the difference in proper motion between the cluster stars and LMC neighbouring stars (and not their absolute values), the systematic offset cancels out. Hence we chose not to correct for this offset ourselves.

The effects and treatment of random (statistical) errors is described in Section 3.

### 2.2 Contamination between Cluster and Surrounding Stars

Our choice of setting the boundary of cluster as  $0.03^\circ$ , and surroundings starting at  $0.05^\circ$  selects nearly the whole cluster in almost all

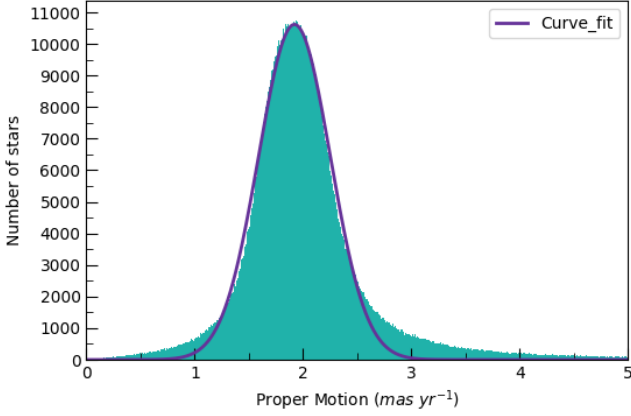


**Figure 1.** Histogram in sea green for the entire sample of LMC stars retrieved, with the best-fit Gaussian overlaid on top in purple

cases as cluster stars, and excludes any cluster stars from our surrounding stars sample. We still qualitatively discuss the effects of one sample contaminating the other.

We observe that our hard boundary of  $0.03^\circ$  does not give the exact boundary of each cluster, though it is a fairly good estimate. Adopting an LMC distance of 50 kpc from Pietrzyński et al. (2013) this corresponds to a radius of about 26 pc. Half-light radii of most globular clusters are about 10 pc or less shown in van den Bergh (2008) while  $r_{90}$  values are on the scale of 20 pc in Werchan & Zaritsky (2011). Tidal radii are on the scale of 20-50 pc for some representative clusters derived in Piatti & Mackey (2018).

Stars of the surrounding star field may get included in the cluster sample and (with a low possibility) vice-versa. This will affect our calculation of mean proper motions. If we assume the proper motions to be random samples drawn from two Gaussians with different means, then we wish to quantify the difference in their means. Contamination will imply that the samples get mixed up, and we end up under-estimating the difference in their means. So with the hard cut, the difference of means that we obtain will be a *lower bound* on the difference of actual mean proper motions rather than the exact difference.

### 3 THE METHOD

Our query for all LMC stars returns about 1.97 million members. We first plot the histogram for proper motion distribution of all the LMC stars with 1000 bins and obtain a smooth Gaussian. The best fit parameters for this Gaussian, obtained by least-squares fitting are  $\mu = 1.92 \pm 0.0015$  mas/year,  $\sigma = 0.109 \pm 0.001$  mas/year. Separating into two coordinates gives us for proper motion along RA,  $\mu_{\alpha*} = \mu_{\alpha} \cos \delta = 1.8338 \pm 0.001$  mas/yr, and  $\mu_{\delta} = 0.3118 \pm 0.001$  mas/yr. This value of  $\mu$  includes the systematic offset which we did not correct for, so has a few percent difference with the values reported in earlier literature in Kallivayalil et al. (2006).

Our aim is to find the difference in the proper motion of the clusters as a whole, with that of the surrounding stars. Under a simplified assumption of all stars having formed in-situ in the galaxy, we expect the cluster stars to have the same mean proper motion as those of the annulus of surrounding blue stars, albeit with small differences that can be attributed as a statistical artifact of our finite sample size in each case. These aforementioned means are obtained from a Gaussian profile fit.

We thus plot histograms for cluster stars and surrounding blue stars (extracted as outlined above) with 100 bins (number of bins is slightly varied to reduce bins that have zero members and can lead to bad fits) and obtain Gaussian features for both cases. Number of cluster stars in our retrieved samples ranged from 85 to 300, and number of surrounding blue stars ranged from about 350 to 5000.

Least-squares fitting with a Gaussian profile is done for both distributions individually using Python's `scipy.optimize.curve_fit` function, and most clusters return an excellent fit with  $< 2\%$  relative error in estimation of mean for cluster stars and  $< 1\%$  for surrounding stars. Those clusters that do not satisfy the above error bound condition are not considered for further analysis, as later work involves differences of a scale that would be rendered insignificant if fitting errors alone are any higher. We found eight clusters that did not pass this criteria, all taken from the list in Bennet et al. (2022). These clusters shared a common characteristic of having low number of cluster as well as surrounding stars (i.e. in sparse surroundings) resultant from a high value of distance from the LMC centre (these distances being reported in the same paper). After noticing this trend we restricted ourselves to clusters closer to the centre, all of which returned good fits.

The Gaussian profiles also indicate that the lack of information of the complete velocity vector (i.e. the line-of-sight velocity) does not significantly hamper our attempt to calculate differences in motion through the galaxy.

From here on, we thus assume that the proper motions of the stars in any of our samples are obtained from a perfectly Gaussian distribution, and any deviation is due to our finite sample size and random errors.

#### 3.1 Statistical Errors

Since we are probing a low-difference regime of proper motions, a proper quantification of the errors in the individual means of cluster and surrounding blue stars is essential. Let  $p_i$  denote the proper motion of the  $i$ -th star, and  $m_p$  denote the mean proper motion of a particular set of stars (which can either be a cluster or blue stars in its surroundings).

For the surrounding stars three sources of errors in the mean are considered:

- The measurement error of proper motion obtained directly from *Gaia*, for each star, denoted as  $\delta p_i$
- The error margin obtained by the curve-fitting (returned by `scipy`), denoted as  $\delta m_{\text{fit}}$
- Since the surrounding blue stars are representative of the local galactic environment, and spanning the LMC disk, the standard deviation of the Gaussian curve-fit is a measure of the randomness in the distribution of stars' proper motion in that local environment. This randomness,  $\sigma_p$  must also be taken into account.

For the total error and confidence interval estimation in the mean  $\Delta m_p$ , we take the root mean square error (RMSE) of measurement errors, the fitting error as it is, and the Gaussian standard deviation scaled down by the sample size of the star set  $N$ . Mathematically,

$$\Delta m_p = \sqrt{\frac{\sum_{i=1}^N \delta p_i^2}{N^2} + \delta m_{\text{fit}}^2 + \frac{\sigma_p^2}{N}}$$

For the globular cluster stars, the Gaussian fit standard deviation,  $\sigma_p$  is a measure of the velocity dispersion which is related to the mass and other physical parameters of the cluster itself - used widely for instance in Hilker et al. (2019), and not related to the stellar motion

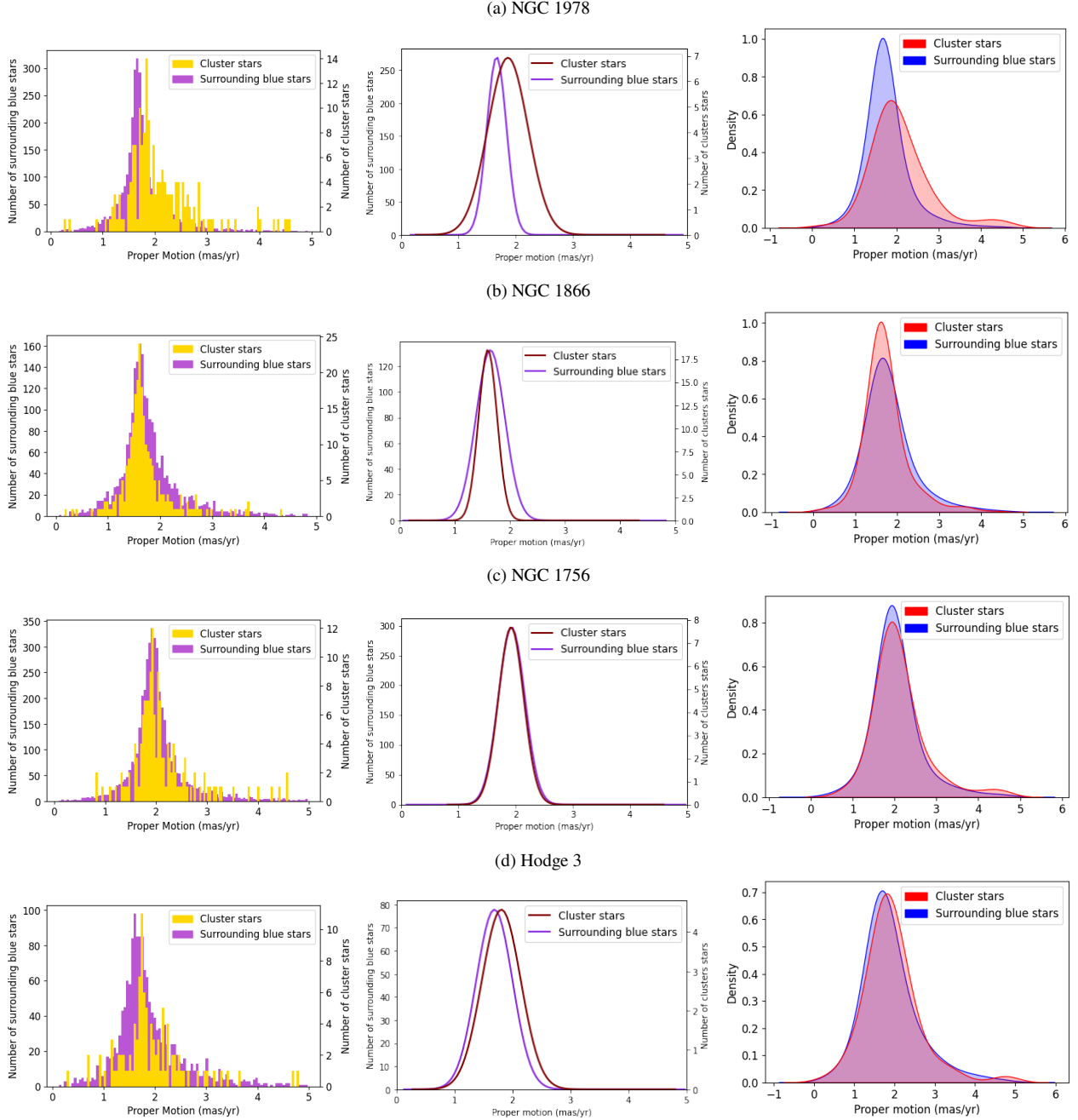


**Figure 2.** Histogram for four clusters from our sample, including their best-fit Gaussians and normalized density plots. For NGC 1978 and Hodge 3 the difference in the peaks of Gaussians i.e. their means, is clearly apparent. For NGC 1756 and NGC 1866 that have smaller difference of means, the difference is minuscule - and can be attributed to shifts due to finite sample size

of the local galactic environment. Therefore, for the error in cluster mean proper motion, only the first two terms are considered in the above sum.

For getting the final confidence interval, we use the following number to quantify the difference of mean proper motions and its significance relative to the errors in means:

$$Q = \frac{|m_{p,cluster} - m_{p,surr}|}{\Delta m_{p,cluster} + \Delta m_{p,surr}}$$

Conversion from  $Q$  to the confidence interval is done using a normal

statistic ( $Q \geq 1$  meaning outside the 68% confidence interval,  $Q \geq 2$  meaning outside the 95% confidence interval, and so on).

For several clusters, we also have the proper motions obtained with a very low error in Table 2 of [Bennet et al. \(2022\)](#), and comparing our obtained mean cluster proper motions with the values reported in the aforementioned paper, we find only a systematic offset ranging between 0.04 mas/yr to 0.09 mas/yr, as we did not correct our values for that. This value of systematic offset is consistent with the representative value of 0.07 mas/yr reported in [Vasiliev \(2019\)](#) for Milky Way's globular clusters.

For finding the absolute difference, we used *our* values of mean



and not those of [Bennet et al. \(2022\)](#), since our means are both uncorrected for the identical systematic error and will hence give the true difference.

### 3.2 Studying Arbitrary Groups of Stars

Globular/open clusters are clearly discernible as point-like overdensities in the outer parts of LMC. However, in the central regions the stellar density appears uniform and we need to ensure that the differences for these clusters aren't a characteristic feature of all stars near the centre. For this we picked arbitrary (RA, Dec) pairs in the central region, and ran the algorithm as described earlier on these patches. The difference increases near the centre to about 0.06 mas/yr but all with  $Q$  less than 1, still small enough to clearly distinguish between the normal and possibly extragalactic globular clusters.

## 4 DISCUSSION

### 4.1 Effect of Errors

The difference in means for the larger fraction for our sample of clusters can be explained by the errors alone, as is evident from the value of  $Q$  being less than 1. We still choose a higher confidence interval of 85% corresponding to  $Q \geq 1.43$ , and segregate those clusters having the above value in a separate class. We also calculate another number for the significance of the mean difference. Since the standard deviation of the Gaussian fit ( $\sigma_{p,surr}$ ) to the surrounding blue stars is a measure of the randomness of stellar motions in that area of the galaxy, we also calculate for all our clusters:

$$D = \frac{|m_{p,cluster} - m_{p,surr}|}{\sigma_{p,surr}}$$

### 4.2 Results for full cluster distribution

We analyzed results for a total of forty-two clusters, spread across throughout the  $5^\circ$  circle around the centre. A majority of the clusters show low values of  $Q$  implying they are following the same path as the LMC's interstellar clouds.

There is a marked gap in the values of  $D$ , between  $D = 0.23$  (equivalent to 18% confidence interval) and  $D = 0.31$  (equivalent to 25% confidence interval). All clusters with  $D \geq 0.31$  also belong to the  $Q \geq 1.43$  group, indicating that the difference of means which is more than 85% significant w.r.t. measurement errors is also on the higher side w.r.t. the dispersion of proper motions in the same environment. One cluster, NGC 2108 has  $D > 0.31$  but  $Q < 1.43$ , though  $Q > 1$  for it might signify it as a significant member too.

It is also interesting to note that except for NGC 2100, all other clusters in the  $Q \geq 1.43$  group are also the only ones to have absolute differences of proper motion  $\geq 0.11$  mas/yr, which at the LMC distance translates to a plane-of-sky velocity difference of about 25 km/s.

### 4.3 Outlier Clusters

The histogram for  $Q$  as shown in the figure follows a clear normal distribution, which means the differences observed are consistent with statistical noise. There is one single outlier at  $Q = 3.5376$ , and its extreme position cannot be explained by noise patterns/distributions alone.

We however chose to study further all the clusters in the  $Q \geq 1.43$

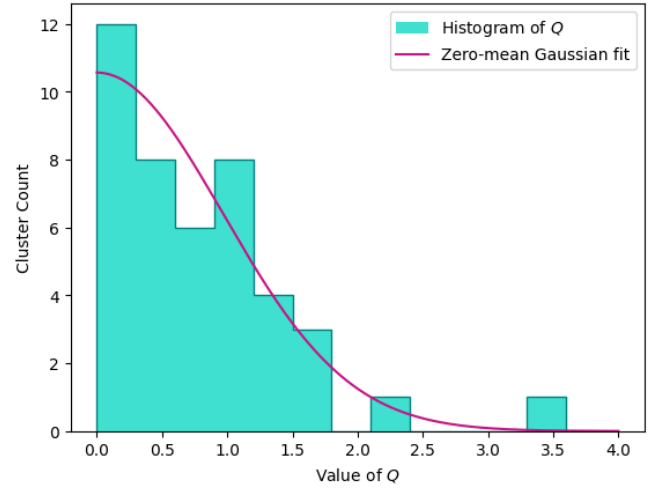


**Figure 3.** Distribution of values of  $Q$  for our cluster sample, as well as a Gaussian profile fit assuming a zero mean. The best-fit standard deviation for this Gaussian is 0.96, close to 1 i.e. the normal distribution. The histogram is consistent with the normal distribution except for a single point at  $Q = 3.5376$ , corresponding to NGC 1978

group. These are NGC 2005, NGC 2210, NGC 1978, Hodge 11, Hodge 3 and NGC 2100. We look at each of these galaxies and review existing literature to argue if these are truly possible extragalactic clusters in LMC. The most spectacular difference as pointed earlier is of NGC 1978, which lies outside the 99% confidence interval in  $Q$ , and outside the 75% confidence interval of  $D$ . Of these six clusters, all except NGC 2100 are globular clusters whose kinematic difference can possibly be ascribed to accretion/disruption events.

We now try to find more properties of our six designated outlier clusters from earlier literature, first reviewing if the only young cluster, NGC 2100, can actually be considered extragalactic in source or not.

**NGC 2100:** This was studied as a young massive cluster in [Patrick et al. \(2016\)](#), and assigned a rough age of 20 Myr therein. It is therefore doubtful if the kinematic difference could be ascribed to an accretion event or not. Its properties have been shown to be similar to its Milky Way counterpart Perseus OB-1, indicating a higher likelihood of it having formed within a galaxy such as LMC. Its age is also consistent with other young clusters of LMC as shown in [Niederhofer et al. \(2015\)](#), further decreasing the probability of it having formed elsewhere. Finally, we mention the absolute difference in proper motion to be lower than 0.11 mas/yr, which is the lower limit for our five other globular clusters. It is entirely possible that the higher  $Q$  value for this cluster arose solely from the low measurement errors in *Gaia*, which is reflected in the error values in the table too. We also note that the surrounding sample for this cluster has a significant portion of the Tarantula Nebula, whose own proper motion dispersion is likely to be low and masking the actual dispersion in the local environment by lowering the value of  $\sigma_{p,surr}$  and increasing  $D$ .

**NGC 2005:** This cluster has the most well-known evidence for the possibility of extragalactic origin as highlighted by chemical analysis in [Mucciarelli et al. \(2021\)](#), although an in-situ origin was also proposed by [Piatti & Hirai \(2023\)](#). It is also an old cluster, as used in [Olszewski et al. \(1996\)](#) and has a low metallicity of -1.54 from [Johnson et al. \(2006\)](#). *In-situ* formation is often associated with higher metallicities as shown by simulation in [Renaud et al. \(2017\)](#), making it a more probable extragalactic candidate.

**NGC 2210:** Earlier evidence for it being an outlier in 3D kinematic

| Name of Cluster | Cluster Mean Proper Motion<br>$m_{p,cluster}$ | Cluster Proper Motion Error<br>$\Delta m_{p,cluster}$ | Surrounding Mean Proper Motion<br>$m_{p,surr}$ | Surrounding Proper Motion Error<br>$\Delta m_{p,surr}$ | Proper Motion Difference | $Q$    | Proper Motion Difference by<br>$\sigma_{p,surr}$ |
|-----------------|---|---|--|--|--------------------------|--------|--|
| NGC 2005        | 2.0051  | 0.0374  | 1.8906   | 0.017  | 0.1145                   | 2.1015 | 0.3194   |
| NGC 1978        | 1.8432  | 0.0446  | 1.6445   | 0.0116   | 0.1988                   | 3.5376 | 1.1522   |
| Hodge 11        | 1.8445  | 0.0579  | 2.0264   | 0.0546   | 0.1819                   | 1.6181 | 0.3567   |
| NGC 2210        | 2.0199  | 0.0493  | 1.8961   | 0.0376   | 0.1238                   | 1.4353 | 0.314  |
| NGC 2100        | 1.9267  | 0.0275  | 1.868  | 0.0114   | 0.0587                   | 1.5087 | 0.3174   |
| Hodge 3         | 1.7872  | 0.0571  | 1.6652   | 0.0231   | 0.122                    | 1.5204 | 0.3904   |
| NGC 1754        | 2.0216  | 0.049   | 1.9827   | 0.0335   | 0.0389                   | 0.4719 | 0.1553   |
| NGC 1786        | 1.8771  | 0.0438  | 1.8067   | 0.0151   | 0.0704                   | 1.1952 | 0.2229   |
| NGC 1835        | 1.9395  | 0.0273  | 1.9677   | 0.0156   | 0.0282                   | 0.6574 | 0.0711   |
| NGC 1916        | 1.9592  | 0.0464  | 1.8901   | 0.0126   | 0.0691                   | 1.1703 | 0.2126   |
| ESO 57-30       | 2.0589  | 0.0397  | 2.1227   | 0.0203   | 0.0638                   | 1.0654 | 0.1397   |
| NGC 2173        | 2.1672  | 0.0482  | 2.2154   | 0.0678   | 0.0482                   | 0.4156 | 0.0948   |
| NGC 2203        | 2.1231  | 0.0615  | 2.0808   | 0.0617   | 0.0424                   | 0.3439 | 0.087  |
| NGC 1928        | 1.9146  | 0.035   | 1.8748   | 0.0113   | 0.0397                   | 0.8582 | 0.1181   |
| NGC 1939        | 2.0451  | 0.0396  | 2.0763   | 0.017  | 0.0311                   | 0.5496 | 0.084  |
| NGC 2108        | 1.8156  | 0.0424  | 1.8799   | 0.0133   | 0.0643                   | 1.1533 | 0.3166   |
| NGC 1806        | 1.8837  | 0.0361  | 1.8365   | 0.0169   | 0.0472                   | 0.8911 | 0.1362   |
| NGC 1903        | 1.9435  | 0.0281  | 1.8927   | 0.0111   | 0.0508                   | 1.2934 | 0.1599   |
| NGC 2214        | 1.816   | 0.0413  | 1.8668   | 0.0316   | 0.0508                   | 0.6969 | 0.1367   |
| NGC 1935        | 1.733   | 0.0323  | 1.6883   | 0.0156   | 0.0448                   | 0.9341 | 0.2244   |
| NGC 1870        | 1.8999  | 0.0359  | 1.8888   | 0.0122   | 0.0111                   | 0.2306 | 0.0295   |
| NGC 2157        | 1.8418  | 0.0409  | 1.8386   | 0.0304   | 0.0032                   | 0.0452 | 0.0118   |
| NGC 2019        | 2.0085  | 0.0352  | 2.0557   | 0.0138   | 0.0472                   | 0.9634 | 0.1204   |
| NGC 1783        | 1.6578  | 0.0461  | 1.6542   | 0.0143   | 0.0036                   | 0.0588 | 0.0165   |
| NGC 1756        | 1.9014  | 0.0416  | 1.9054   | 0.0102   | 0.004                    | 0.0774 | 0.0172   |
| NGC 1805        | 1.6057  | 0.0419  | 1.6227   | 0.0134   | 0.017                    | 0.3067 | 0.0765   |
| NGC 1818        | 1.6276  | 0.0407  | 1.6768   | 0.0171   | 0.0492                   | 0.8514 | 0.1669   |
| NGC 1831        | 1.7276  | 0.0315  | 1.6574   | 0.0266   | 0.0702                   | 1.2085 | 0.228  |
| NGC 1866        | 1.579   | 0.0266  | 1.6217   | 0.0166   | 0.0427                   | 0.9906 | 0.1627   |
| NGC 1898        | 2.0416  | 0.0314  | 1.9745   | 0.0207   | 0.0671                   | 1.2873 | 0.1998   |
| NGC 1987        | 2.1418  | 0.0353  | 2.1886   | 0.0196   | 0.0468                   | 0.8529 | 0.1214   |
| NGC 2031        | 2.1675  | 0.0336  | 2.1738   | 0.0168   | 0.0063                   | 0.1248 | 0.0226   |
| NGC 2156        | 1.8027  | 0.0438  | 1.8059   | 0.018  | 0.0033                   | 0.0527 | 0.0134   |
| NGC 2159        | 1.8064  | 0.0417  | 1.8042   | 0.0167   | 0.0023                   | 0.0386 | 0.0098   |
| NGC 1712        | 1.9255  | 0.0337  | 1.9147   | 0.016  | 0.0109                   | 0.2189 | 0.0435   |
| NGC 1755        | 1.8586  | 0.0343  | 1.8472   | 0.0182   | 0.0114                   | 0.2164 | 0.0375   |
| NGC 1763        | 1.7089  | 0.0388  | 1.7286   | 0.0152   | 0.0197                   | 0.3652 | 0.1014   |
| NGC 1846        | 1.777   | 0.0369  | 1.7753   | 0.0208   | 0.0017                   | 0.0289 | 0.005  |
| NGC 1847        | 1.8405  | 0.0382  | 1.8722   | 0.0165   | 0.0318                   | 0.5808 | 0.0919   |
| NGC 1854        | 1.9173  | 0.0316  | 1.9112   | 0.0134   | 0.0061                   | 0.1354 | 0.0191   |
| NGC 1711        | 1.9518  | 0.0324  | 1.9538   | 0.0127   | 0.002                    | 0.0445 | 0.0085   |
| NGC 1944        | 2.1388  | 0.0472  | 2.1791   | 0.0313   | 0.0402                   | 0.5125 | 0.1142   |
| NGC 2121        | 2.0127  | 0.0384  | 2.0787   | 0.0197   | 0.066                    | 1.1367 | 0.171  |

**Table 1.** The set of clusters covered in this study, along with the properties analyzed. Derivation for each quantity has been elucidated in previous sections. All proper motions and differences, errors are in mas/yr. The last column highlights the difference of proper motion means as a fraction of the Gaussian-fit standard deviation of the surrounding blue stars (denoted as  $D$  henceforth), as an alternate estimate to  $Q$  of how far the means are statistically. Our six clusters were chosen with  $Q \geq 1.43$  corresponding to lying outside the 85% confidence interval, as well as having  $D \geq 0.31$ , corresponding to outside the 25% confidence interval

space is given by [Bennet et al. \(2022\)](#), who also pointed to its possible extragalactic origin, and is also an old cluster studied in [Olszewski et al. \(1996\)](#). [Gilligan et al. \(2019\)](#), and later [Gilligan et al. \(2020\)](#) showed that NGC 2210 and Hodge 11 are the only two clusters to show multiple populations in horizontal branch. Multiple populations can be seen as cores of accreted dwarf galaxies as shown in [Helmi \(2008\)](#), though we acknowledge the presence of multiple populations in several globular clusters, and hence not a unique property of the subset we have.

**Hodge 3:** No significant properties were found in earlier literature that can serve as evidence for it to be a cluster of extragalactic origin.

**Hodge 11:** Like NGC 2210, [Gilligan et al. \(2019\)](#) showed it had

multiple stellar populations, including those in horizontal branch. Both of these also have the most heavily populated blue-straggler branch among the old clusters studied by [Wagner-Kaiser et al. \(2017\)](#) as seen in their HR diagrams. Both of these, combined with their spatial closeness, suggests a common pathway of evolution and possibly a common origin to both, which may be attributed to an accretion event.

**NGC 1978:** This has been known to be a highly elliptical globular cluster, quite unlike most Milky Way GCs as shown in [Mucciarelli et al. \(2007\)](#). High ellipticity of LMC clusters in general was associated to the weak tidal field of LMC compared to the Milky Way in [Goodwin \(1997\)](#) that preserves the original triaxial structure of

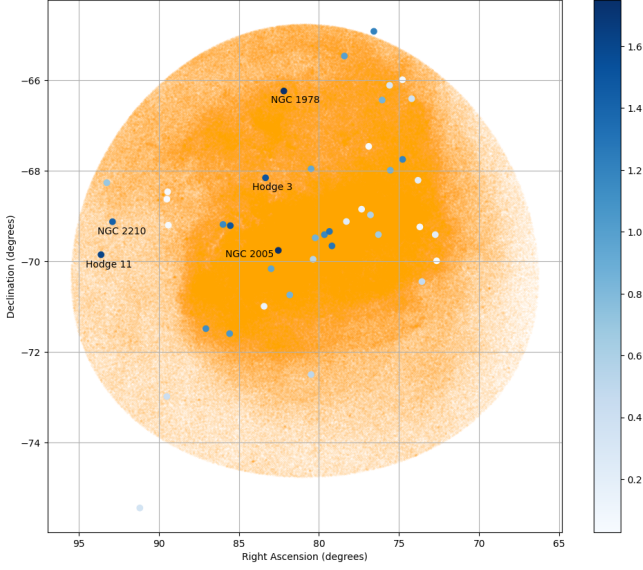


**Figure 4.** Distribution of the clusters studied in this work in the Large Magellanic Cloud, with the colour intensity equal to the  $Q$  value whose calculation is given in 3.1. Colour value is clipped at 1.75 for better contrast. Names of the five outlier clusters and coordinate grids are also present. We notice our five clusters lying preferentially to the North-East.

clusters. We propose that the extra higher ellipticity of NGC 1978 may have been a result of it having formed originally in a dwarf galaxy, and being accreted into the LMC much later, thus giving tidal forces less time to make it closer to spherical. Ferraro et al. (2006) also showed that the ellipticity is not a result of merging of two clusters/gas clouds. Metallicity and ages of several clusters was studied by Narloch et al. (2022), who commented that NGC 1978, despite being significantly older than the surrounding field population, has a slightly greater metallicity ( $-0.38$  for cluster vs  $-0.44$  for field), which should have been lower if it was born in the same region in an earlier epoch. This combined with the large deviation in mean proper motion, suggests that it formed in a different environment.

#### 4.4 Spatial Position

The rotational period of LMC stars around its centre as determined by van der Marel & Kallivayalil (2014) is 250 million years. This renders it impossible for us to determine the exact direction from which the clusters may have been accreted or disrupted in their paths, though simulations and further data refinement might make it possible. We still see our outlier clusters all roughly lying in the North-Eastern part of LMC, which also contains the Tarantula Nebula. We calculate the position angles for each of the five clusters w.r.t. the centre of LMC at (RA, Dec) = (80.8942, -69.756) using the standard convention; northwards is the  $0^\circ$  line and angle is measured positive to East of North. The values of position angles (in degrees) for each cluster is given in Table 2.

In contrast, the position angle of the Tarantula Nebula is  $63.46^\circ$ , which is quite close to the average PA of the clusters at  $60.1^\circ$ . All of them lie in the same quadrant as the Nebula. We suggest that the same activity that resulted in the disruption of cluster motions may also have accelerated its star formation activity.

| Cluster Name | Position Angle |
|--------------|----------------|
| NGC 2005     | $89.8^\circ$   |
| NGC 1978     | $8.43^\circ$   |
| Hodge 3      | $29.2^\circ$   |
| NGC 2210     | $81.55^\circ$  |
| Hodge 11     | $91.2^\circ$   |

**Table 2.** Position Angles of the five outlier clusters w.r.t. LMC centre

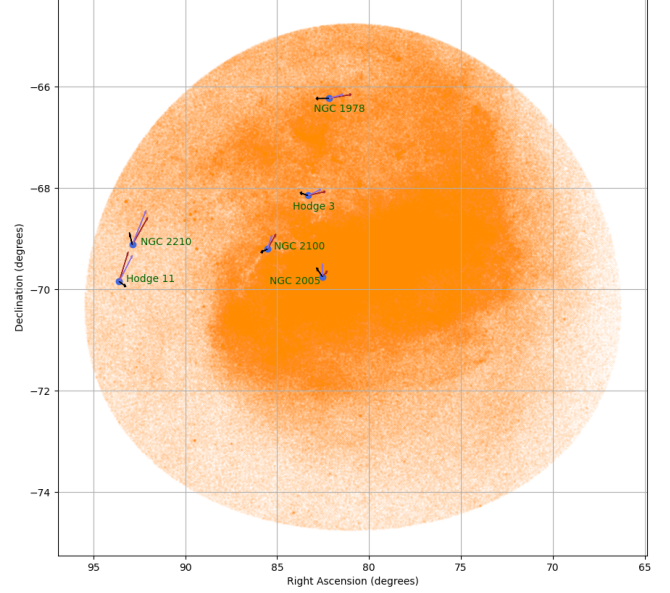


**Figure 5.** Relative proper motions of each of the clusters and their surrounding blue stars w.r.t. the mean motion of LMC, represented as arrows. Violet arrows show the cluster proper motion, brown ones show that of the surrounding stars and the black arrows show the difference. Lengths of arrows are proportional to the values of proper motions, with black arrows all scaled up by 33% for better visibility

| Cluster Name | Angle of Proper Motion Difference |
|--------------|-----------------------------------|
| NGC 2005     | $33.56^\circ$                     |
| NGC 2210     | $13.9^\circ$                      |
| Hodge 3      | $70.83^\circ$                     |
| NGC 1978     | $90.42^\circ$                     |
| Hodge 11     | $231.47^\circ$                    |
| NGC 2100     | $118.33^\circ$                    |

**Table 3.** Position Angles of the five outlier clusters w.r.t. LMC centre

#### 4.5 Direction of Proper Motion Differences

We resolve the proper motions of the six clusters as well as their surrounding blue stars beyond  $Q \geq 1.43$  into its two components,  $\mu_\alpha \cos \delta$  and  $\mu_\delta$ . The relative motions w.r.t. the mean motion of LMC (found earlier in 3) are taken, and these values are used to calculate the difference in each of the components of the proper motion. A representative image is shown in Figure 5.

The general trend of rotational velocity of LMC stars is evident from the direction of arrows. The direction of the difference (black arrows) can be computed as their position angle (standard convention of northwards being the  $0^\circ$  line and angle measured positive to East of North). The angles are shown in Table 3.

Four of the five globular clusters lying in the  $Q \geq 1.43$  group have their difference position angles lying inside an approximately  $80^\circ$  interval from  $12^\circ$  to  $92^\circ$ . Comparing with the earlier derived values

| Cluster Name | $Q_{cluster,blue}$ | $Q_{cluster,red}$ | $Q_{blue,red}$ |
|--------------|--------------------|-------------------|----------------|
| NGC 2005     | 2.1015             | 1.5113            | 1.7545         |
| NGC 2210     | 1.4353             | 2.0817            | 0.0887         |
| Hodge 3      | 1.5204             | 0.0413            | 3.7811         |
| NGC 1978     | 3.5376             | 3.3123            | 1.0513         |
| Hodge 11     | 1.6181             | 1.4448            | 1.2029         |
| NGC 2100     | 1.5087             | 2.3801            | 1.3845         |

**Table 4.** Values of  $Q$  between cluster stars, blue (young) surrounding stars, and red (old) surrounding stars

of clusters' position angles, we find both NGC 1978 and Hodge 3 (lying to the North) having a slower rotation speed than the stellar disk and the difference PA close to  $80^\circ$ . NGC 2100 loosely follows the above as well, however the nature of its proper motion difference with stellar disk is more questionable given previous literature.

NGC 2005 and NGC 2210 both lie Eastward and have a faster rotation speed and a difference PA close to  $20^\circ$ . The trend cannot be robustly ascertained given we have only two data points for each of them. However, if it is of physical origin, it might point to two separate events to explain their nature. Hodge 11 has its difference pointed nearly antiparallel to that of its closest neighbour NGC 2210, which again may or may not have an underlying physical reason.

#### 4.6 Comparison with Surrounding Red Stars

For our six clusters with  $Q \geq 1.43$ , we also try to compare the cluster proper motion with that of the surrounding red ( $G_{BP} - G_{RP} > 0.75$ ) stars (i.e. the older stellar population of the local LMC disk). We report the values of  $Q$ , the difference significance in mean proper motions of the cluster with blue stars, the cluster with red stars, and the red stars with blue stars, respectively in Table 4

We see that for two clusters, NGC 2210 and NGC 2100,  $Q$  increases when the cluster motion is compared to the red stars instead of the blue ones. Since NGC 2100 is a young cluster, this result is expected. For NGC 2210, the error in mean proper motion of red stars was much less than that for the blue stars, which reflects in the high  $Q$ . The absolute values of the differences are nearly similar, and the similarity of proper motions in blue and red surrounding stars reflects in the very low  $Q_{red,blue} = 0.09$ .

For the four other clusters,  $Q$  decreases when we compare cluster stars with red disk stars instead of the blue disk stars. This may be explained by the possible accretion/disruption event bringing in a smaller population of old stars itself apart from the cluster, and mixing with the existent LMC disk's old population. The most marked reduction of  $Q$  happened for Hodge 3.

$Q_{blue,red}$  in general has high values ( $> 1$ ), even though the absolute values of proper motion differences are all  $< 0.06$  mas/yr (except Hodge 3, where it is  $0.12$  mas/yr), mainly due to the fact that the star sample size of disk stars have higher numbers, bringing down the effect of random errors significantly.

## 5 CONCLUSIONS

We examined the proper motions of several clusters and quantified the difference of cluster proper motions with that of young, blue stars in their surroundings and examined their significance w.r.t. errors in the determined means. Major results can be summarized as below:

(i) The majority of clusters have very small differences, with a value of  $Q \leq 1$  which can be accounted for by errors alone.

(ii) Systematic errors cancel out when taking a difference. Statistical errors in the mean are quantified accounting for measurement errors in *Gaia*, Gaussian fitting error as well as the Gaussian standard deviation of proper motions in the surrounding star sample. The values of the metric  $Q$ , which represents the significance of mean proper motion difference over the sum of errors, follows a roughly normal Gaussian distribution except NGC 1978 which is a clear outlier and whose difference cannot be accounted for by statistical error distributions alone.

(iii) We use a cut of 85% confidence interval of  $Q$  to separate clusters with significantly different mean proper motions from their surroundings.

(iv) This group had five globular clusters with relatively higher proper motion differences  $> 0.11$  mas/yr (equivalent to physical plane-of-sky velocity difference  $> 25$  km/s), and a sixth young cluster. Literature review for these six clusters provides contrary evidence to extragalactic origin for the young cluster, but a moderate corroboration for our hypothesis that the old globulars may either be accreted or have been affected by some significant disruption event by a nearby interacting galaxy. Correlations between positions and direction of differences may point to two distinct events.

We mainly aim this work to serve as observational evidence of the five clusters having a different proper motion from the rest of their surroundings, although the normal distribution of  $Q$  shows that this difference may or may not have a physical origin. Only in the case of NGC 1978, the clear presence of a physically different proper motion can be ascertained. A direct cause of this could be a galaxy accretion/disruption event; however, further work such as simulations, more precise astrometric and spectral analyses are essential to confirm the true reason for the difference.

## ACKNOWLEDGEMENTS

We extend our sincerest gratitude to the referee for their patient scrutiny and detailed comments that immensely helped to improve the analysis of errors and statistical significance of differences. We would also like to thank Himanshu Verma, PhD in Physics, IIT Bombay and Kritika, the astronomy club of IIT Bombay for giving us the first exposure to analyzing data from *Gaia*, without which this project would have been impossible. This work has used data from the European Space Agency (ESA) mission *Gaia* (<https://sci.esa.int/web/gaia>), processed by the Gaia Data Processing and Analysis Consortium (DPAC, <https://www.cosmos.esa.int/web/gaia/dpac/consortium>). Funding for the DPAC has been provided by national institutions, in particular the institutions participating in the Gaia Multilateral Agreement.

## DATA AVAILABILITY

This work used public data available via *astroquery.Gaia*, the Python API to access *Gaia* DR3 data. Processing of spacecraft data is carried out by DPAC.

## REFERENCES

- Battaglia G., Taibi S., Thomas G. F., Fritz T. K., 2022, *Astronomy & Astrophysics*, 657, A54
- Bennet P., Alfaro-Cuello M., del Pino A., Watkins L. L., van der Marel R. P., Sohn S. T., 2022, *The Astrophysical Journal*, 935, 149



- Bica E. L. D., Schmitt H. R., Dutra C. M., Oliveira H. L., 1999, *The Astrophysical Journal*, 117, 238
- Carretta E., et al., 2010, *The Astrophysical Journal*, 714, L7
- Dreyer J. L. E., 1888, *Mem. RAS*, 49, 1
- Erkal D., Belokurov V. A., 2020, *Monthly Notices of the Royal Astronomical Society*, 495, 2554
- Ferraro F. R., Mucciarelli A., Carretta E., Origlia L., 2006, *The Astrophysical Journal*, 645, L33
- Gaia Collaboration 2016, *Astronomy & Astrophysics*, 595, A1
- Gaia Collaboration 2022, Gaia Data Release 3: Summary of the content and survey properties, [doi:10.48550/arXiv.2208.00211](https://arxiv.org/abs/10.48550/arXiv.2208.00211)
- Gilligan C. K., et al., 2019, *Monthly Notices of the Royal Astronomical Society*, 486, 5581
- Gilligan C. K., et al., 2020, *Monthly Notices of the Royal Astronomical Society*, 494, 1946
- Goodwin S. P., 1997, *Monthly Notices of the Royal Astronomical Society: Letters*, 286, L39
- Helmi A., 2008, *The Astronomy and Astrophysics Review*, 15, 145
- Helmi A., Babusiaux C., Koppelman H. H., Massari D., Veljanoski J., Brown A. G. A., 2018a, *Nature*, 563, 85
- Helmi A., van Leeuwen F., McMillan P. J., Massari D., Antoja T., Robin A. C., 2018b, *Astronomy & Astrophysics*, 616, A12
- Hilker M., Baumgardt H., Sollima A., Bellini A., 2019, *Proceedings of the International Astronomical Union*, 14, 451
- Hodge P. W., Wright F. W., 1967, The Large Magellanic Cloud
- Johnson J. A., Ivans I. I., Stetson P. B., 2006, *The Astrophysical Journal*, 640, 801
- Kallivayalil N., van der Marel R. P., Alcock C., Axelrod T., Cook K. H., Drake A. J., Geha M., 2006, *The Astrophysical Journal*, 638, 772
- Lindegren L., Hernández J., Bombrun A., Klioner S., and U. B., 2018, *Astronomy & Astrophysics*, 616, A2
- Lindegren L., Klioner S. A., Hernández J., et al. 2021, *Astronomy & Astrophysics*, 649, A2
- Massari D., Koppelman H. H., Helmi A., 2019, *Astronomy & Astrophysics*, 630, L4
- Mucciarelli A., Ferraro F. R., Origlia L., Pecci F. F., 2007, *The Astronomical Journal*, 133, 2053
- Mucciarelli A., Massari D., Minelli A., Romano D., Bellazzini M., Ferraro F. R., Matteucci F., Origlia L., 2021, *Nature Astronomy*, 5, 1247
- Narloch W., et al., 2022, *Astronomy & Astrophysics*, 666, A80
- Niederhofer F., Hilker M., Bastian N., Silva-Villa E., 2015, *Astronomy & Astrophysics*, 575, A62
- Olszewski E. W., Suntzeff N. B., Mateo M., 1996, *Annual Review of Astronomy and Astrophysics*, 34, 511
- Pagnini G., Matteo P. D., Khoperskov S., Mastrobuono-Battisti A., Haywood M., Renaud F., Combes F., 2023, *Astronomy & Astrophysics*, 673, A86
- Patel E., et al., 2020, *The Astrophysical Journal*, 893, 121
- Patrick L. R., Evans C. J., Davies B., Kudritzki R.-P., Hénault-Brunet V., Bastian N., Lapenna E., Bergemann M., 2016, *Monthly Notices of the Royal Astronomical Society*, 458, 3968
- Piatti A. E., Hirai Y., 2023, *The Astronomical Journal*, 165, 213
- Piatti A. E., Mackey A. D., 2018, *Monthly Notices of the Royal Astronomical Society*, 478, 2164
- Pietrzyński G., et al., 2013, *Nature*, 495, 76
- Ramos P., et al., 2022, *Astronomy & Astrophysics*, 666, A64
- Renaud F., Agertz O., Gieles M., 2017, *Monthly Notices of the Royal Astronomical Society*, 465, 3622
- Sollima A., 2020, *Monthly Notices of the Royal Astronomical Society*, 495, 2222
- Vasiliev E., 2019, *Monthly Notices of the Royal Astronomical Society*, 484, 2832
- Wagner-Kaiser R., et al., 2017, *Monthly Notices of the Royal Astronomical Society*, 471, 3347
- Werchan F., Zaritsky D., 2011, *The Astronomical Journal*, 142, 48
- van den Bergh S., 2008, *Monthly Notices of the Royal Astronomical Society: Letters*, 385, L20
- van der Marel R. P., Kallivayalil N., 2014, *The Astrophysical Journal*, 781, 121

## APPENDIX

This paper has been typeset from a  $\text{\LaTeX}$  file prepared by the author.

| Name of Cluster | Right Ascension (J2000)<br>in hh mm ss | Declination (J2000)<br>in dd mm ss | Number of Stars<br>in Cluster | Number of<br>Surrounding Blue Stars | Proper Motion<br>(this work) | Proper Motion in<br><a href="#">Bennet et al. (2022)</a> |
|-----------------|--|------------------------------------|-------------------------------|-------------------------------------|------------------------------|--|
| NGC 2005        | 05 30 08.500                           | -69 45 14.42                       | 198                           | 1607                                | 2.01 ± 0.04                  | ...  |
| NGC 1978        | 05 28 45.330                           | -66 14 12.04                       | 167                           | 3246                                | 1.84 ± 0.04                  | 1.8 ± 0.01   |
| Hodge 11        | 06 14 22.92                            | -69 50 54.9                        | 97                            | 529                                 | 1.84 ± 0.06                  | 1.77 ± 0.04  |
| NGC 2210        | 06 11 31.296                           | -69 07 17.04                       | 101                           | 709                                 | 2.02 ± 0.05                  | 2.07 ± 0.07  |
| NGC 1754        | 04 54 18.080                           | -70 26 32.58                       | 112                           | 2181                                | 2.02 ± 0.05                  | ...  |
| NGC 1786        | 04 59 07.470                           | -67 44 45.44                       | 131                           | 3407                                | 1.88 ± 0.04                  | 1.95 ± 0.1   |
| NGC 1835        | 05 05 09.210                           | -69 24 20.96                       | 245                           | 3991                                | 1.94 ± 0.03                  | ...  |
| NGC 1916        | 05 18 37.87                            | -69 24 22.9                        | 231                           | 2263                                | 1.96 ± 0.05                  | ...  |
| ESO 57-30       | 05 42 17.300                           | -71 35 27.47                       | 152                           | 2431                                | 2.06 ± 0.04                  | ...  |
| NGC 2173        | 05 57 58.0                             | -72 58 42                          | 85                            | 543                                 | 2.17 ± 0.05                  | 2.13 ± 0.04  |
| NGC 2203        | 06 04 42.0                             | -75 26 18                          | 101                           | 472                                 | 2.12 ± 0.06                  | ...  |
| NGC 2100        | 05 42 07.200                           | -69 12 26.99                       | 201                           | 3142                                | 1.93 ± 0.03                  | ...  |
| Hodge 3         | 05 33 19.700                           | -68 09 07.23                       | 101                           | 1554                                | 1.79 ± 0.06                  | ...  |
| NGC 1928        | 05 20 55.940                           | -69 28 34.96                       | 252                           | 4068                                | 1.91 ± 0.03                  | 1.89 ± 0.01  |
| NGC 1939        | 05 21 26.82                            | -69 56 59.0                        | 241                           | 1595                                | 2.05 ± 0.04                  | 1.99 ± 0.01  |
| NGC 2108        | 05 43 56.270                           | -69 10 54.37                       | 148                           | 2468                                | 1.82 ± 0.04                  | 1.8 ± 0.01   |
| NGC 1806        | 05 02 11.180                           | -67 59 05.89                       | 195                           | 3153                                | 1.88 ± 0.04                  | 1.81 ± 0.01  |
| NGC 1903        | 05 17 22.700                           | -69 20 08.17                       | 266                           | 4295                                | 1.94 ± 0.03                  | ...  |
| NGC 2214        | 06 12 57.0                             | -68 15 36                          | 147                           | 880                                 | 1.82 ± 0.04                  | ...  |
| NGC 1935        | 05 21 58.0                             | -67 57 18                          | 183                           | 2001                                | 1.73 ± 0.03                  | ...  |
| NGC 1870        | 05 13 08.920                           | -69 06 59.62                       | 262                           | 4414                                | 1.9 ± 0.04                   | ...  |
| NGC 2157        | 05 57 35.430                           | -69 11 48.67                       | 134                           | 797                                 | 1.84 ± 0.04                  | ...  |
| NGC 2019        | 05 31 56.48                            | -70 09 32.5                        | 233                           | 3405                                | 2.01 ± 0.04                  | ...  |
| NGC 1783        | 04 59 08.590                           | -65 59 15.84                       | 177                           | 2415                                | 1.66 ± 0.05                  | 1.65 ± 0.01  |
| NGC 1756        | 04 54 49.130                           | -69 14 10.20                       | 147                           | 4397                                | 1.9 ± 0.04                   | 1.86 ± 0.01  |
| NGC 1805        | 05 02 21.690                           | -66 06 39.43                       | 146                           | 3281                                | 1.61 ± 0.04                  | -  |
| NGC 1818        | 05 04 13.300                           | -66 26 05.47                       | 177                           | 2852                                | 1.63 ± 0.04                  | 1.53 ± 0.03  |
| NGC 1831        | 05 06 17.4                             | -64 55 11                          | 178                           | 913                                 | 1.73 ± 0.03                  | 1.8 ± 0.11   |
| NGC 1866        | 05 13 38.920                           | -65 27 52.75                       | 246                           | 2263                                | 1.58 ± 0.03                  | 1.58 ± 0.05  |
| NGC 1898        | 05 16 45.380                           | -69 39 16.76                       | 263                           | 389                                 | 2.04 ± 0.03                  | ...  |
| NGC 1987        | 05 27 16.940                           | -70 44 14.16                       | 195                           | 2436                                | 2.14 ± 0.04                  | 2.06 ± 0.01  |
| NGC 2031        | 05 33 41.440                           | -70 59 14.54                       | 202                           | 2545                                | 2.17 ± 0.03                  | ...  |
| NGC 2156        | 05 57 45.0                             | -68 27 36                          | 115                           | 1542                                | 1.8 ± 0.04                   | ...  |
| NGC 2159        | 05 57 57.0                             | -68 37 24                          | 126                           | 1496                                | 1.81 ± 0.04                  | 1.78 ± 0.07  |
| NGC 1712        | 04 50 58.0                             | -69 24 24                          | 188                           | 1882                                | 1.93 ± 0.03                  | ...  |
| NGC 1755        | 04 55 16.390                           | -68 12 23.12                       | 196                           | 1708                                | 1.86 ± 0.03                  | ...  |
| NGC 1763        | 04 56 51.5                             | -66 24 25                          | 148                           | 1743                                | 1.71 ± 0.04                  | ...  |
| NGC 1846        | 05 07 34.900                           | -67 27 32.45                       | 207                           | 1976                                | 1.78 ± 0.04                  | ...  |
| NGC 1847        | 05 07 08.200                           | -68 58 15.49                       | 224                           | 2376                                | 1.84 ± 0.04                  | ...  |
| NGC 1854        | 05 09 21.180                           | -68 50 39.56                       | 298                           | 2787                                | 1.92 ± 0.03                  | ...  |
| NGC 1711        | 04 50 37.320                           | -69 59 01.72                       | 216                           | 3109                                | 1.95 ± 0.03                  | ...  |
| NGC 1944        | 05 21 57.466                           | -72 29 38.60                       | 118                           | 762                                 | 2.14 ± 0.05                  | ...  |
| NGC 2121        | 05 48 13.190                           | -71 28 52.00                       | 164                           | 2275                                | 2.01 ± 0.04                  | ...  |

**Table 5.** Properties of our Cluster Sample. Proper Motions are in mas/yr